



# Lowermost mantle flow at the eastern edge of the African Large Low Shear Velocity Province



Heather A. Ford<sup>\*</sup>, Maureen D. Long, Xiaobo He<sup>1</sup>, Colton Lynner

Department of Geology and Geophysics, Yale University, New Haven, CT, USA

## ARTICLE INFO

### Article history:

Received 19 January 2015

Received in revised form 11 March 2015

Accepted 13 March 2015

Available online 28 March 2015

Editor: P. Shearer

### Keywords:

anisotropy

shear wave splitting

D''

LLSVP

post-perovskite

## ABSTRACT

Observations of seismic anisotropy in the lowermost mantle are plentiful, but their interpretation in terms of mantle flow remains challenging. Here we interrogate the anisotropic structure of the lowermost mantle beneath the Afar region, just outside the edge of the African Large Low Shear Velocity Province, using a combination of shear wave splitting techniques applied to phases propagating at five distinct raypath orientations. We then model the resulting data set by testing various candidate mechanisms for anisotropy. The observations are best fit by a model that invokes the lattice preferred orientation (LPO) of post-perovskite, with the [100] crystallographic axis oriented either nearly vertically or highly obliquely to the horizontal plane. Plausible corresponding mantle flow scenarios involve a significant vertical flow component, which suggests that the African Large Low Shear Velocity Province edge may deflect ambient mantle flow upwards or may be associated with a sheet-like upwelling.

© 2015 Elsevier B.V. All rights reserved.

## 1. Introduction

The African Large Low Shear Velocity Province (LLSVP) is a well-established feature of global tomography models and, in combination with the Pacific LLSVP, dominates the seismic structure of the lower mantle (e.g., Lekic et al., 2012). The properties, origin, dynamics, and longevity of LLSVPs are debated (e.g., Davies et al., 2012). Specifically, it is unclear whether LLSVPs are long-lived, stable structures that anchor mantle dynamics (Dziewonski et al., 2010) or whether they represent passive structures aggregated by subduction-driven flow above the CMB (McNamara and Zhong, 2005). The sides of LLSVPs are thought to be seismically sharp and steeply dipping (e.g., Ni et al., 2002; Wang and Wen, 2007; Sun and Miller, 2012), and their margins may represent possible zones of plume generation (Torsvik et al., 2008).

Observations of seismic anisotropy are often used to shed light on dynamic processes in the Earth's mantle. Seismic anisotropy is commonly observed in the upper mantle, while the bulk of the lower mantle is generally thought to be isotropic (Meade et al., 1995). The D'' layer at the base of the mantle is an exception (e.g., Kendall and Silver, 1996; Panning and Romanowicz, 2006); observations of anisotropy in the lowermost mantle are

<sup>\*</sup> Corresponding author at: Department of Geology and Geophysics, Yale University, PO Box 208109, New Haven, CT 06520-8109, USA.

E-mail address: heather.ford@yale.edu (H.A. Ford).

<sup>1</sup> Now at: Ocean College, Zhejiang University, Hangzhou, China.

abundant (Nowacki et al., 2011), but their relationship to mantle dynamics remains unclear. There is debate over whether D'' anisotropy is the result of lattice-preferred orientation (LPO) of one or more mineral phases or the shape-preferred orientation (SPO) of elastically distinct material such as partial melt (Karato, 1998; Nowacki et al., 2011). Uncertainty also exists over the mineralogical composition of the lowermost mantle (which may vary laterally; e.g., Cobden et al., 2012) and whether the dominant mineral phase is MgSiO<sub>3</sub> perovskite (bridgmanite) or its high-pressure post-perovskite (ppv) polymorph.

Most body wave studies of D'' anisotropy are effectively limited to a single set of (usually horizontal) raypaths, due to the uneven distribution of sources and receivers at the Earth's surface, with a few exceptions (Wookey and Kendall, 2008; Nowacki et al., 2010). When regions of D'' are sampled from a single orientation, it hampers our ability to distinguish among the different possible mechanisms for lowermost mantle anisotropy, as the anisotropic geometry is not tightly constrained. Here, we overcome this common observational limitation by interrogating a single region of D'' just outside the edge of the African LLSVP (Fig. 1) using a combination of splitting techniques applied to rays propagating at five distinct orientations. This observational strategy allows us to constrain the anisotropic geometry more tightly than possible with a single propagation direction. The methods and results of our shear wave splitting analysis are described in Section 2. We then implement a set of mineral-physics based forward models that test a variety of elastic tensors and orientations that correspond to a range of potential mantle flow scenarios, as discussed in Section 3.

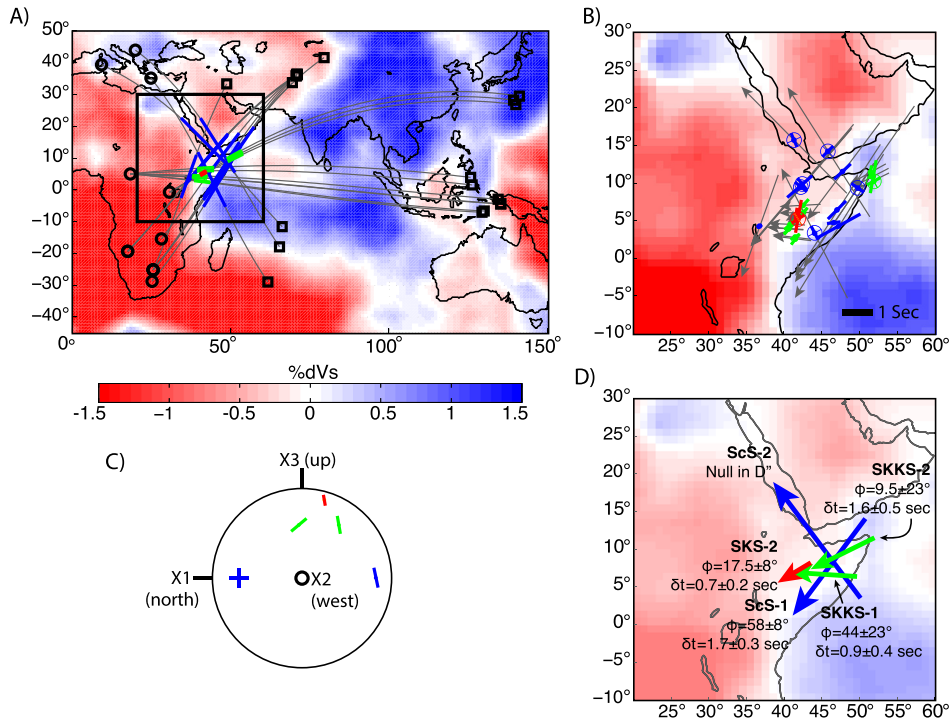


**Fig. 1.** (A) Raypaths used in this study (gray lines), with event (squares) and station (circles) locations. Thick solid lines indicate portions of the raypaths sampling D'' for ScS (blue), SKKS (green) and SKS (yellow). Background colors indicate S velocity anomalies at 2650–2900 km depth from the GYPsuM tomography model (Simmons et al., 2010). (B) Individual splitting measurements for ScS (blue), SKKS (green) and SKS (yellow), plotted at the midpoint of the D'' portion of the raypath (gray arrows). Orientation and length of the bars correspond to  $\phi$  (clockwise from north) and  $\delta t$  (in seconds), respectively, as measured at the station. Circles with cross-hairs indicate null arrivals, with initial polarization direction (thick line). (C) Spherical projection of raypath-averaged  $\phi$ , using the same plotting convention as in later figures. (D) Schematic of raypath-averaged splitting parameters. Arrows correspond to the average raypaths of ScS (blue), SKKS (green) and SKS (yellow) through D''. SKS and SKKS path lengths are exaggerated (2 $\times$ ) for clarity. Groups ScS-1, ScS-2, SKKS-1 and SK(K)S-2 are referred to in Tables 1 and 2. (For interpretation of the references to color in this figure legend, the reader is referred to the web version of this article.)

This allows us to discriminate which mechanisms and orientations are compatible with the observations. Finally, the range of permissible models is interpreted in terms of plausible mantle flow scenarios at the edge of the African LLSVP (Section 4).

## 2. Shear wave splitting: methods and results

### 2.1. Station selection and measurement methods

We present measurements for SKS, SKKS, and ScS phases recorded at stations in Africa and Europe that sample a region just outside the African LLSVP beneath the Afar region (Fig. 1). Our study region was carefully selected such that the raypaths sample a region of D'' just outside the LLSVP edge, with little or no sampling of structure within the LLSVP itself. Just to the south of our study area, the location of the LLSVP edge has been well constrained via waveform modeling techniques (Wang and Wen, 2004), but directly beneath Afar the best constraints on the location of the structure's edge come from tomographic models. In particular, the cluster analysis of Lekic et al. (2012) demonstrates that the LLSVP boundary here is relatively well constrained, although there is some uncertainty given the imperfect resolution of global tomographic models.

We measure splitting over a range of raypath propagation directions using differential S–ScS (Wookey et al., 2005a, 2005b; Wookey and Kendall, 2008; Nowacki et al., 2010) and discrepant SKS–SKKS splitting (Niu and Perez, 2004; Long, 2009; He and Long, 2011; Lynner and Long, 2014). Each of these methods relies on a thorough characterization of upper mantle anisotropy beneath the seismic station so that the effects of receiver-side anisotropy can be properly accounted for. In this study, we restricted our analysis to stations which met two criteria, following Lynner and

Long (2013): 1) good backazimuthal coverage for SK(K)S phases that was sufficient to evaluate the presence of complex anisotropy (multiple anisotropic layers, dipping symmetry axes) beneath the receiver, and 2) SK(K)S splitting patterns that reflect either a lack of splitting at the frequencies examined in this study, or simple splitting that indicates the presence of a single horizontal layer of anisotropy beneath the station.

A total of 9 stations were selected for use in this study: BGCA, BOSA, DIVS, IDI, LBTB, LSZ, MBAR, TSUM, and VSL. SK(K)S splitting patterns for several of these stations at the frequencies of interest were documented previously by Lynner and Long (2014), while stations DIVS and VSL were newly evaluated for this study. One station used here (MBAR) has been previously categorized as “complex” for the purpose of characterizing source-side anisotropy beneath subduction zones (Lynner and Long, 2013). However, MBAR exhibits null SKS arrivals over a large swath of backazimuths, including all four backazimuthal quadrants, and only a few non-null SK(K)S measurements, most of which are associated with discrepant SKS–SKKS pairs. For the purpose of this study, therefore, we have characterized MBAR as a “null” station with little or no splitting associated with upper mantle anisotropy beneath the receiver; we attribute the complex (discrepant) SKS–SKKS splitting to D'' anisotropy in our study region. Station locations and associated upper mantle anisotropy corrections can be found in Tables 1 and 2.

Differential S–ScS splitting measurements were carried out using the method of Wookey et al. (2005a, 2005b). Briefly, this method uses the difference in splitting between direct S waves (which do not sample the D'' layer) and ScS waves (which propagate nearly horizontally through D'') to isolate the contribution to splitting from the lowermost mantle. We selected events of magnitude  $M_w \geq 5.5$  at epicentral distances between 60° and 85° for

Download English Version:

<https://daneshyari.com/en/article/6428153>

Download Persian Version:

<https://daneshyari.com/article/6428153>

[Daneshyari.com](https://daneshyari.com)